ISBN: 978-3-95450-233-2 ISSN: 2673-5504 doi:10.18429/JACoW-SRF2021-WEPTEV013

NEW FREQUENCY-TUNING SYSTEM AND DIGITAL LLRF FOR STABLE AND RELIABLE OPERATION OF SRILAC

K. Suda*, O. Kamigaito, K. Ozeki, N. Sakamoto, K. Yamada
RIKEN Nishina Center, Wako, Japan
E. Kako, H. Nakai, H. Sakai, K. Umemori, KEK, Tsukuba, Japan
H. Hara, A. Miyamoto, K. Sennyu, T. Yanagisawa
Mitsubishi Heavy Industries Machinery Systems, Ltd. (MHI-MS), Kobe, Japan

Abstract

The superconducting booster linac at RIKEN (SRILAC) has ten 73-MHz quarter-wavelength resonators (QWRs) that are contained in three cryomodules. The beam commissioning of SRILAC was successfully performed in January 2020. Frequency tuning during cold operation is performed by compressing the beam port of the cavity with stainless wires and decreasing the length of each beam gap, similar to the method adopted at ANL and FRIB. However, each tuner is driven by a motor connected to gears, instead of using gas pressure. Since the intervals of the QWRs are small due to the beam dynamics, a compact design for the tuner was adopted. Each cavity was tuned to the design frequency, which required frequency changes of 3 kHz to 7 kHz depending on the cavity. Although no piezoelectric actuator is mounted on the tuning system, phase noise caused by microphonics can be sufficiently reduced by a phase-locked loop using a newly developed digital LLRF. The details of the tuning system as well as the digital LLRF will be presented.

INTRODUCTION

The RIKEN heavy-ion linac (RILAC), consisted of normal conducting cavities [1–3], was used to accelerate intense ion beams to synthesize super-heavy elements Nh [4]. RILAC has been upgraded to allow further investigations of super-heavy elements and production of radioactive isotopes by introducing a new ECR ion source and a superconducting booster linac (SRILAC) [5]. The beam commissioning was performed successfully in January 2020. The SRILAC has ten quarter-wavelength resonators (QWRs) made of bulk niobium (Nb) contained in three cryomodules (Fig. 1). Quadrupole magnets are located in warm sections outside the cryomodules. In order to maintain a good beam quality and to limit the space taken up by cryomodules in the existing accelerator hall, the length of each cryomodule had to be minimized. The distance between the beam port flanges of the cavity in the cryomodules was set to as small as 110 mm. Since frequency tuning during cold operation is performed by compressing the beam ports [6], a compact mechanism for the frequency tuner was required.

* ksuda@ribf.riken.jp

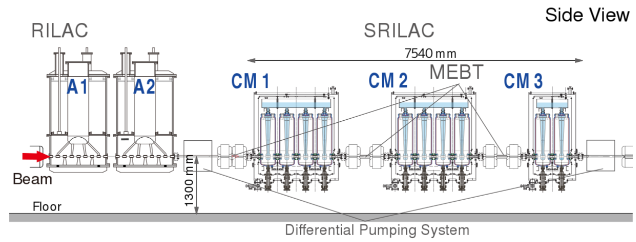

Figure 1: Schematic layout of the SRILAC and the last part of the RILAC. CM1–3: cryomodules, A1&A2: normal conducting cavities for RILAC. Quadrupole doublets are located in the Medium Energy Beam Transport line (MEBT).

FREQUENCY TUNING SYSTEM

Requirements of Tuner

Figure 2 shows a schematic view of a cavity with a titanium (Ti) jacket. Note that no stiffener was installed in the stem. The figure also shows a permalloy local magnetic shield with a thickness of 1.5 mm, which is put on a bare cavity before jacketing so that the magnetic shield is installed between the cavity and jacket. We chose a capacitive tuning method that decreases the frequency by compressing the beam ports, as mentioned above, and fabricated cavities so that the frequency is higher than the operating frequency by a few kHz when the tuner is free at cold temperatures. The tuner is used to decrease the frequency by a few kHz at the beginning of cavity excitation, as well as compensating the frequency shift by a few Hz caused by fluctuations of helium pressure. Based on the regulations regarding high-pressure gas safety in Japan, the cavities were designed to be rigid. We adopted a conical stem and fabricated the cavities from niobium sheet with a thickness of 3.5 or 4 mm. Although the stiffness helps to decrease the effects of microphonics, the required force of the tuner to change the frequency by −14 kHz is as high as 7.5 kN for each beam port, with a maximum displacement of 0.37 mm as determined from a simulation [6]. The simulation result of the displacement by a force applied perpendicular to the face of a beam port flange is shown in Fig. 3.

Tuner Mechanism

To fulfill the requirements mentioned above, the tuner mechanism was designed and fabricated by MHI-MS. Figure 4 shows the tuner mechanism assembled on a cryomodule. Each beam port of a cavity is pressed with a force less

ISBN: 978-3-95450-233-2 ISSN: 2673-5504 doi:10.18429/JACoW-SRF2021-WEPTEV013

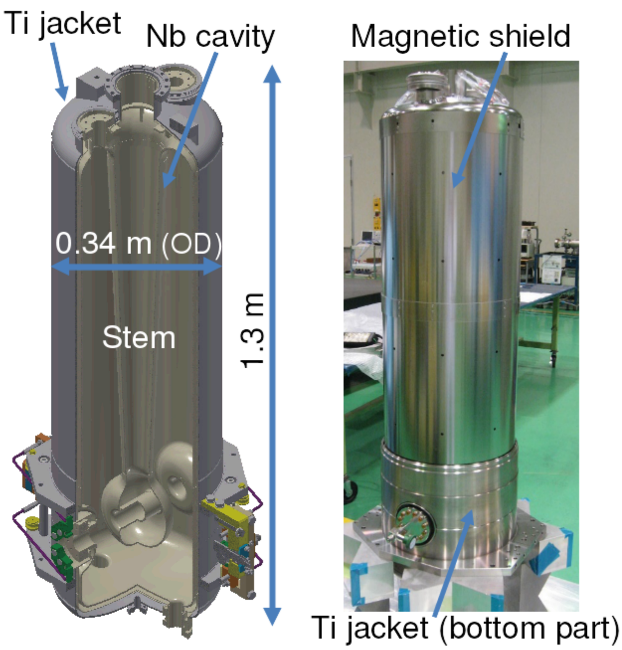

Figure 2: Schematic view of a cavity (left panel) and a picture of a magnetic shield put on a bare cavity before jacketing (right panel).

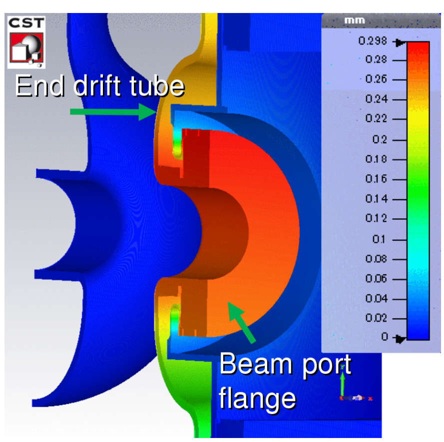

Figure 3: Simulation result of displacement by a force applied to the face of a beam port flange.

than 10 kN by pulling two ϕ10 mm stainless steel wires. A drive plate, to which four wires are connected, is driven through a shaft with a feed per revolution of 2 mm/rev. The shaft is rotated by a stepping motor through a three-stage gearbox, where each gear ratio is 4:1 and the total gear ratio is 64:1. A rotary encoder is attached to the second gear. A magnetic fluid vacuum seal is attached in the gear box. No piezoelectric actuator is attached on the system. A tuner mechanism utilizing wires is not unique, ANL developed a pneumatic tuner which used helium pressure to actuate the tuning mechanism [7, 8], and FRIB adopted a similar system for a half-wavelength resonator [9]. However, MHI-MS obtained patents for their system that employs supporting plates and pulleys (see Fig. 4) to actuate the mechanism [10].

Tuner Test at 4.5 K

After the cryomodules were assembled and installed, cooling tests were carried out from September 2019 [5]. During the tests, the frequencies of the cavities at 4.5 K were measured by a network analyzer in October and November. Port 1 was connected to the coupler and port 2 to the cavity pickup, and the input power was +0 dBm. All the tuners were set to be free. The results are shown by purple circles in Fig. 5. Frequency shifts of 3 kHz to 7 kHz were required, depending on the cavity, at an operation frequency of 73 MHz. Starting from these frequencies, by rotating the drive shaft of the tuner, each cavity was smoothly tuned to the operation frequency successfully (Fig. 6), demonstrating that the frequency tuning during the fabrication process [6] was appropriate and the tuning mechanism works well.

Although hysteresis was observed when the tuners were released, the differences in the frequencies were only +0.2–+0.6 kHz. This indicates that there was no plastic deformation.

LOW-LEVEL RF CONTROL SYSTEM

The RF control system consists of a digital feedback module (LLRF), solid-state amplifier with a maximum output power of 7.5 kW, transmission line with directional couplers (to monitor the forward power P_{in} and reflected power P_{ref}), fundamental power coupler (PC), cavity pickup, tuner controller, and motor for the tuner (Fig. 7(upper panel)). The amplifier is equipped with built-in isolators.

The hardware design of the digital LLRF for SRILAC is almost identical to that developed for the 75.5-MHz prototype cavity [11], except for an FPGA chip and additional circuits to enable faster communication with an upper control device. The number of available logic gates was doubled by upgrading the Xilinx XC6SLX75 chip to XC6SLX150 for the purpose of implementing additional functionality in the future.

A PID feedback loop control is implemented in the software for the voltage and phase of the cavity pickup signal. Excitation of the cavities is performed by manual control. A self excited loop (SEL) mode is used for startup and the system is then switched to a generator driven (GD) mode. Three 16-bit analog-to-digital converter (ADC, Analog Devices AD9446) are used to digitize the input signals by I-Q under sampling at a frequency of $f_0 \times 4/5$ MHz (=58.4 MHz), where f_0 = 73 MHz (Fig. 7(lower panel)). A 14-bit direct digital synthesizer (DDS, Analog Devices AD9957BSVZ) operates as a digital-to-analog converter (DAC) at a frequency of $f_0 \times 8$ MHz (=584 MHz) to output RF signals. The difference in the phases between P_{in} and P_{ref} is processed and provided to the tuner controller for automatic tuning.

In high-power tests, the feedback parameters were adjusted to decrease phase noise. Figure 8 shows the spectra of a cavity pickup signal in the GD mode. The feedback control reduced the phase noise well.

ISBN: 978-3-95450-233-2 ISSN: 2673-5504 doi:10.18429/JACoW-SRF2021-WEPTEV013

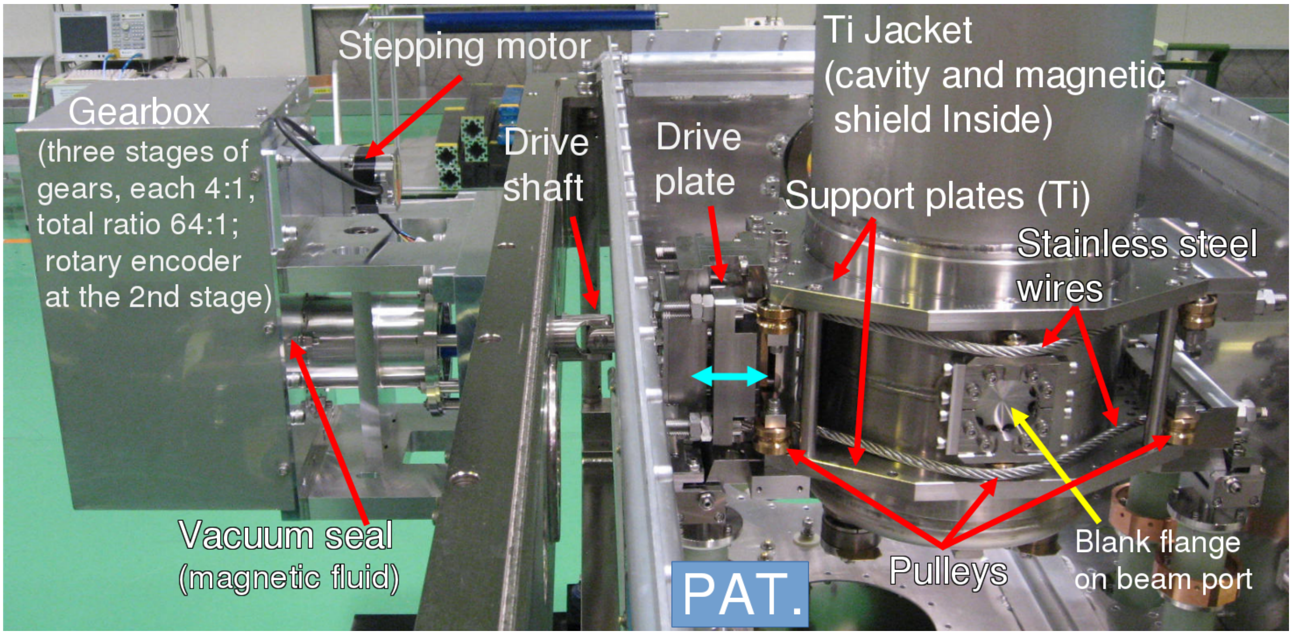

Figure 4: Tuner mechanism assembled on a cryomodule.

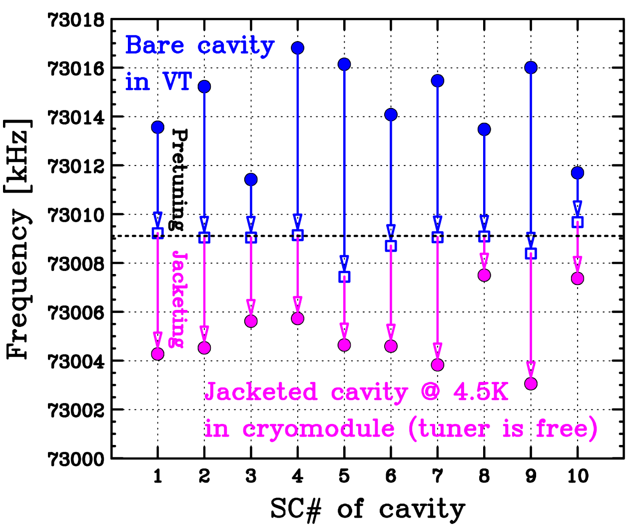

Figure 5: Frequencies of the ten cavities. The blue circles show the data from vertical tests (VT) at 4.2 K performed in 2018. The blue squares are estimates taken by summing the VT results and the pretuning frequency shifts [6]. The purple circles show data at 4.5 K obtained during cooling tests of the cryomodules in 2019.

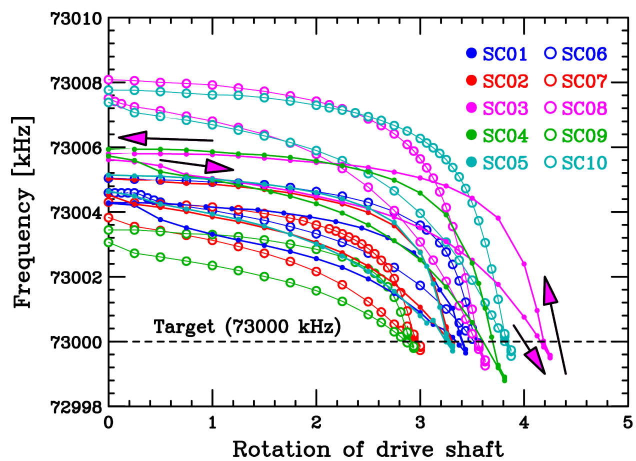

Figure 6: Frequencies measured during cooling tests of cryomodules.

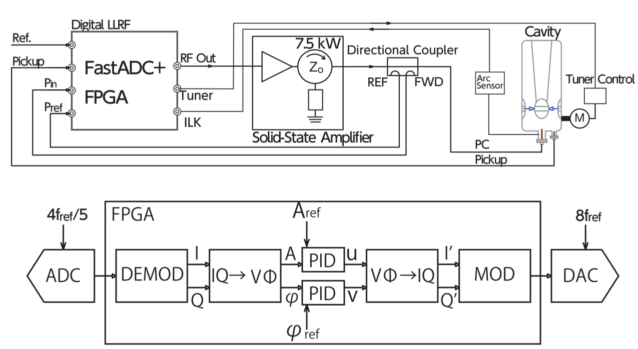

Figure 7: Block diagram of the RF control system (upper panel) and digital low-level RF system (lower panel).

SENSITIVITY OF FREQUENCY AGAINST HELIUM PRESSURE

A sudden increase of helium pressure was observed during a high-power test in January 2021 (Fig. 9). This seems to have been due to excess heating at the top torus of one cavity (SC02) caused by a high gap voltage of 1800 kV in the GD mode. Since the other cavities in CM1 were excited in the SEL mode, their frequencies were measured. From these data, the frequency sensitivity of the cavity against helium

ISBN: 978-3-95450-233-2 ISSN: 2673-5504 doi:10.18429/JACoW-SRF2021-WEPTEV013

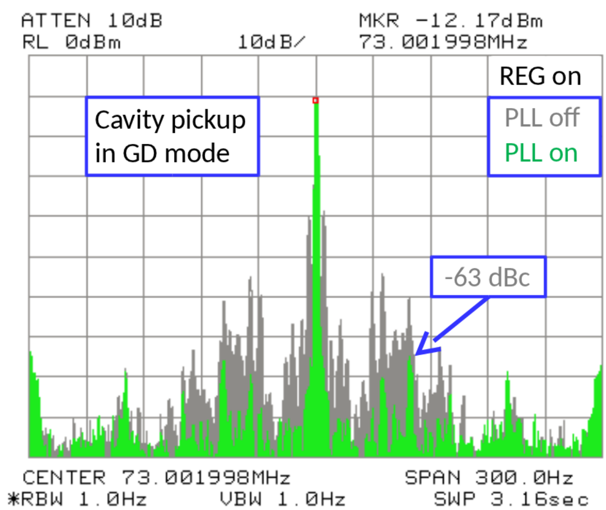

Figure 8: Spectra of a cavity pickup signal when the phase-locked loop (PLL) was off (gray) and on (green) in the GD mode.

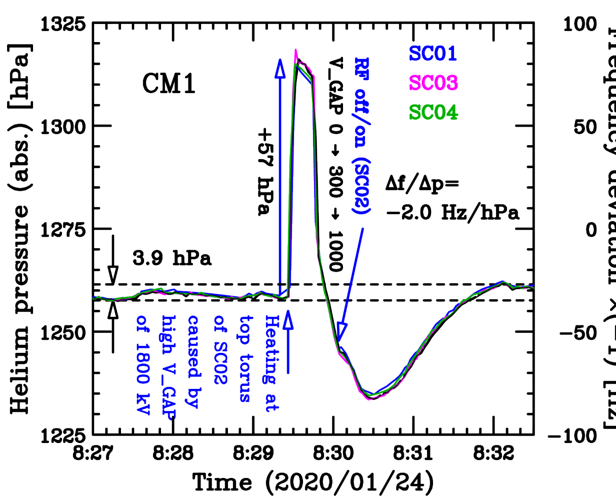

Figure 9: Helium pressure (black solid curve) and deviations of cavity frequencies (colored lines for SC01, SC03, SC04) measured during a high-power test.

pressure was determined to be $\Delta f/\Delta p = 2.0$ Hz/hPa. This value is in good agreement with the simulation result of −1.9 Hz/hPa [6]. Figure 10 shows the stability of the helium pressure as well as the cavity frequencies. The pressure was well controlled by a refrigerator within $|\Delta p| < 4.3$ hPa over a day. This corresponds to a frequency deviation as small as $|\Delta f| < 9$ Hz, and is less than 1/2×(bandwidth of cavity) (=25 Hz). However in some cases, larger fluctuations of helium pressure occurred a few times per day, the cause of which has not yet been identified.

AUTOMATIC TUNING CONTROL

For long-term operation, automatic tuning control was introduced to compensate the variations in the cavity frequency. The tuner is driven proportional to the phase difference between P_{in} and P_{ref} (+offset) if the difference exceeds a dead

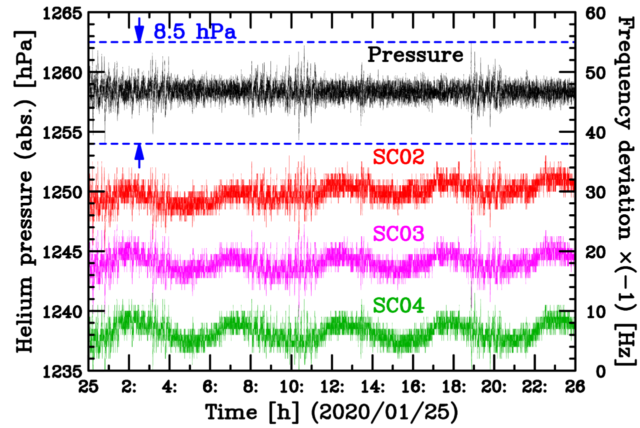

Figure 10: Stability of helium pressure and cavity frequencies over a day.

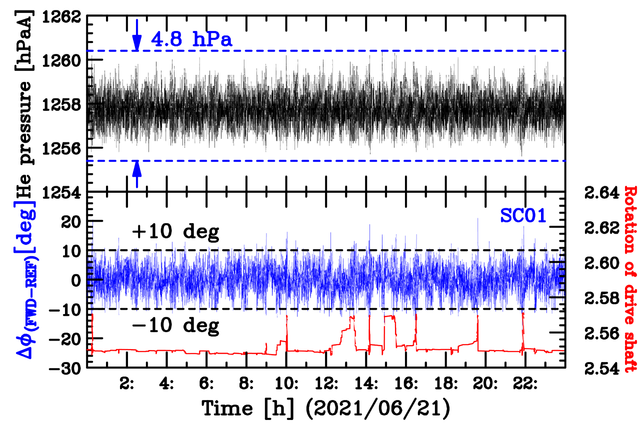

Figure 11: Helium pressure (upper panel), phase difference $\Delta\phi$ between P_{in} and P_{ref}, and rotation of the tuner drive shaft (lower panel). The tuner was driven if $\Delta\phi$ exceeded a dead zone of ±10 degrees.

band. Here, the dead band was set to be ±10 degrees to mitigate hysteresis (backlash) of ∼ 10 Hz (Fig. 11).

SUMMARY

A compact tuner for the cavities of SRILAC was designed, and the mechanisms were assembled in cryomodules. All the cavities were smoothly tuned to the operation frequency in cooling tests of the cryomodules carried out in 2019. Automatic tuning control was successfully introduced in 2020 for long-term operation.

REFERENCES

[1] M. Odera *et al.*, "Variable frequency heavy-ion linac, RILAC: I. Design, construction and operation of its accelerating structure", *Nucl. Instrum. Methods Phys. Res., Sect. A*, vol. 227, pp. 187–195, 1984. doi:10.1016/0168-9002(84)90121-9

[2] O. Kamigaito *et al.*, "Construction of a variable-frequency radio-frequency quadrupole linac for the RIKEN heavy-ion linac", *Rev. Sci. Instrum.*, vol 70, pp. 4523–4531, 1999. doi:10.1063/1.1150105

ISBN: 978-3-95450-233-2 ISSN: 2673-5504 doi:10.18429/JACoW-SRF2021-WEPTEV013

[3] O. Kamigaito *et al.*, “Construction of a booster linac for the RIKEN heavy-ion linac”, *Rev. Sci. Instrum.*, vol 76, p. 013306, 2005. doi:10.1063/1.1834708

[4] K. Morita *et al.*, “Experiment on the synthesis of Element 113 in the reaction ^{209}Bi(^{70}Zn,n)^{278}113”, *J. Phys. Soc. Jpn.*, vol. 73, pp. 2593–2596, 2004. doi:10.1143/JPSJ.73.2593

[5] K. Yamada *et al.*, “Successful beam commissioning of heavy-ion superconducting linac at RIKEN”, presented at SRF’21, Grand Rapids, MI, USA, Jun. 2021, paper MOOFAV01, this conference.

[6] K. Suda *et al.*, “Fabrication and performance of superconducting quarter-wavelength resonators for SRILAC”, in *Proc. SRF’19*, Dresden, Germany, Jun. 2019, pp. 182–187. doi:10.18429/JACoW-SRF2019-MOP055

[7] M. Kelly *et al*, “Microphonics in the ATLAS upgrade cryomodule”, in *Proc. SRF’09*, Berlin, Germany, Sep. 2009, paper TUPPO031, pp. 269–272.

[8] R. Paparella, “Overview of recent tuner development on elliptical and low-beta cavities”, in *Proc. SRF’15*, Whistler, BC, Canada, Sep. 2015, paper FRAA01, pp. 1425–1431.

[9] K. Saito *et al.*, “SRF Developments at MSU for FRIB”, in *Proc. SRF’13*, Paris, France, Sep. 2013, paper MOP013, pp. 106–111.

[10] H. Hara and K. Sennyu, Japanese Patent No. 5985011 B1, 2016; *id.*, European Patent No. 3319404 A1, 2018; *id.*, U.S. Patent No. 10383204 B2, 2019.

[11] N. Sakamoto *et al.*, “Development of superconducting quarter-wave resonator and cryomodule for low-beta ion accelerators at RIKEN radioactive isotope beam factory”, in *Proc. SRF’19*, Dresden, Germany, Jun. 2019, pp. 750–757. doi:10.18429/JACoW-SRF2019-WETEB1